



# Assimilating multi-source uncertainties of a parsimonious conceptual hydrological model using hierarchical Bayesian modeling

Wei Wu<sup>a,\*</sup>, James S. Clark<sup>b</sup>, James M. Vose<sup>c</sup>

<sup>a</sup> Nicholas School of the Environment, Box 90328, Duke University, Durham, NC 27708, USA

<sup>b</sup> Nicholas School of the Environment and Department of Biology, Box 90328, Duke University, Durham, NC 27708, USA

<sup>c</sup> USDA-Forest Service, Coweeta Hydrologic Laboratory, 3160 Coweeta Lab Road, Otto, NC 28763, USA

## ARTICLE INFO

### Article history:

Received 17 September 2009

Received in revised form 1 August 2010

Accepted 23 September 2010

This manuscript was handled by Andras Bardossy, Editor-in-Chief, with the assistance of Fi-John Chang, Associate Editor

### Keywords:

Hierarchical Bayesian modeling

Hydrological modeling

Soil moisture

Streamflow

## SUMMARY

Hierarchical Bayesian (HB) modeling allows for multiple sources of uncertainty by factoring complex relationships into conditional distributions that can be used to draw inference and make predictions. We applied an HB model to estimate the parameters and state variables of a parsimonious hydrological model – GR4J – by coherently assimilating the uncertainties from the model, observations, and parameters at Coweeta Basin in western North Carolina. A state-space model was within the Bayesian hierarchical framework to estimate the daily soil moisture levels and their uncertainties.

Results show that the posteriors of the parameters were updated from and relatively insensitive to priors, an indication that they were dominated by the data. The uncertainties of the simulated streamflow increased with streamflow increase. By assimilating soil moisture data, the model could estimate the maximum capacity of soil moisture accounting storage and predict storm events with higher precision compared to not assimilating soil moisture data. This study has shown that hierarchical Bayesian model is a useful tool in water resource planning and management by acknowledging stochasticity.

© 2010 Elsevier B.V. All rights reserved.

## 1. Introduction

Hydrologic models are used to assess how quantity and the quality of water will be influenced by environmental conditions. Data-driven precipitation-runoff models are used to simulate hydrological cycles, to fill the gaps in streamflow records, and to forecast future soil moisture content and water yield under different scenarios of climate and land use/land cover changes. Because some key parameters of the model cannot be obtained by physical measurements, it is necessary to fit the model's outputs to time series of observations, usually streamflow, and sometimes in combination with soil moisture. In this paper we demonstrate how a hierarchical Bayes model can be used to assimilate soil moisture and stream flow data to better understand hydrological processes.

Soil moisture data should be directly integrated into hydrological models, because soil moisture provides a connection between physical processes at the catchment scale and biological processes at finer scales. Soil moisture is determined by precipitation, evapotranspiration, infiltration, percolation and runoff, and it has major impacts on a range of hydrological processes including flooding, erosion, solute transport (Western et al., 2004). Soil moisture data

are used by hydrologists to understand runoff, including effects of land-use practice on hydrological processes (Blume et al., 2007) and by ecologists to understand tree growth, soil biogeochemical processes, and energy exchange between land and atmosphere. Subsurface storm flow (fast lateral subsurface flow) is affected by soil type, biological activity, precipitation characteristics and soil water content (Kienzler and Naef, 2007). Soil moisture is also likely to control near stream saturated areas that produce saturation excess overland flow when a large precipitation event occurs (van Meerveld and McDonnell, 2005). Thus assimilating soil moisture data in hydrological models has potential to increase predictability of storm events.

The many mechanisms involved in connecting precipitation and streamflow can motivate detailed hydrological models, often with large numbers of parameters. However, fitting many parameters in large models is often limited by data. Additional parameters and complex structure can demand unrealistic calibration efforts without necessarily leading to an improved fit, in part due to poorly identified parameters. On the other hand, simple models with four or five parameters based on a quick-flow and slow-flow conceptualization usually provide an adequate fit to daily streamflow data (Jakeman and Hornberger, 1993; Kuczera and Mroczkowski, 1998).

As with any model driven by multiple sources of information, uncertainty in hydrological models is large and must be acknowledged in predictions to balance complexity with performance. However, many of the historical methods are based on optimization

\* Corresponding author. Present address: Department of Coastal Sciences, The University of Southern Mississippi, 703 East Beach Drive, Ocean Springs, MS 39564, USA. Tel.: +1 228 818 8855; fax: +1 228 818 8848.

E-mail address: [wei.wu@usm.edu](mailto:wei.wu@usm.edu) (W. Wu).

and provide point estimates of parameters and point predictions, rather than uncertainties. In recent years considerable confusion and debate have focused on the various ad hoc techniques applied to data assimilation and uncertainty quantification. For multiple data sets, many of the widely used models are inconsistent. For example, Mantovan and Todini (2006) point out that Generalized Likelihood Uncertainty Estimator (GLUE) is not coherent. The assumption of independent observations allows us to model the joint likelihood as a product of likelihoods for individual observations. Autoregressive structures accommodate serial dependence within a time series, but not between multiple types of observations that enter models in a variety of ways. Coherent treatment of uncertainty is possible where conditional independence is imposed at the data stage, with stochasticity at the process stage to describe known (deterministic) and unknown (stochastic) dependence (Clark, 2007). Stochasticity at the process stage allows us to focus on conditional independence at the 'data' stage, and take up the relationships among state variables at the 'process' stage, still tractable when decomposed into a hierarchical structure. As an alternative to a simple AR structure, with limited capacity to describe interactions among variables and uncertainties, we discuss a hierarchical Bayes approach and show its utility for integrating observations on stream flow and soil moisture, within a non-linear model having process uncertainty.

Recent advances in computation, i.e., Markov chain Monte Carlo (MCMC), facilitate Bayesian inference in hydrological studies (Kuczera and Parent, 1998; Campbell et al., 1999; Bates and Campbell, 2001; Marshall et al., 2004). MCMC simulation generates a sample of latent variables and parameters to produce a Markov chain that converges to a stationary distribution. The simulated posterior distribution can be summarized, in terms of uncertainties on parameters and latent states (Bates and Campbell, 2001) and used to construct predictive distributions (Clark et al., 2001).

In this study, we implemented a hierarchical Bayesian model to estimate the parameters, latent variables, and uncertainties in streamflow predictions for a conceptual hydrological model by applying MCMC simulation techniques. In particular, we assessed the effect of inclusion of soil moisture data on the precision of streamflow predictions, especially during precipitation events.

## 2. Methods

### 2.1. Site description

We studied two control watersheds (Watersheds 18 and 27) at the Coweeta Hydrological Laboratory in the Nantahala Mountain Range of western North Carolina within the Blue Ridge Physiographic Province (35°03'N, 83°25'W) (Fig. 1). The Coweeta Basin of 1626 ha has been a center of forest hydrological research in the mountains-piedmont of Georgia, South Carolina, North Carolina, and Virginia since 1934 and has been a National Science Foundation (NSF) Long Term Ecological Research Site since 1980 (Swank and Crossely Jr., 1988). Climate at Coweeta Basin is marine humid temperate and characterized by cool summers, mild winters and abundant rainfall in all seasons (Swift et al., 1988). Average annual precipitation varies from 1700 mm at low elevations (680 m) to 2500 mm on upper slopes (>1400 m). The hydrology is dominated by rain events, snow usually comprises less than 5% of the precipitation. The underlying bedrock is the Coweeta group (Hatcher Jr., 1979), which consists of quartz diorite gneiss, metasandstone and pelitic schist, and quartzose metasandstone (Hatcher Jr., 1988). The regolith of the Coweeta Basin is deeply weathered and averages about 7 m in depth.

Watershed 18 (WS18 12.5 ha) and Watershed 27 (WS27 38.8 ha) support mixed hardwoods. Both watersheds serve as ref-

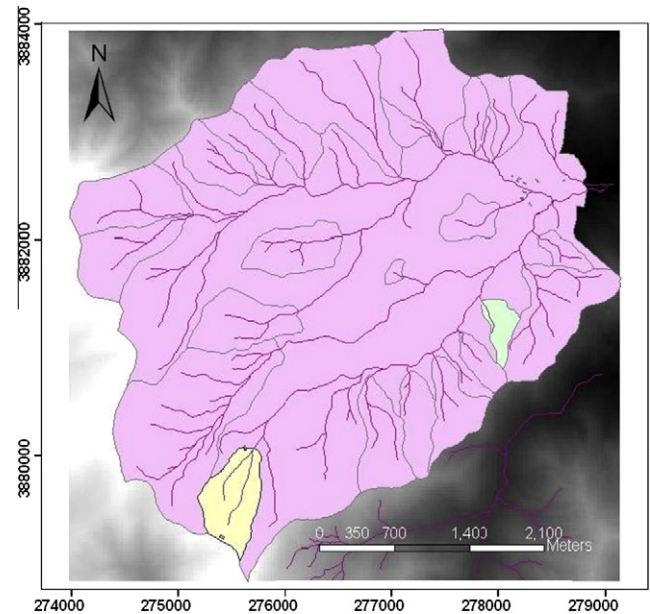


**Fig. 1.** Coweeta Basin with stream network (purple lines) and major watersheds (gray line as boundary) including Watershed 18 (green area) and 27 (yellow area) which we have focused on in this study (coordinate system: Universal Transverse Mercator (UTM) in meters). (For interpretation of the references to colour in this figure legend, the reader is referred to the web version of this article.)

erence watersheds and have been unmanaged since being selectively logged in the early 1900s. The elevation of Watershed 18 ranges from 726 to 993 m.a.s.l with an average slope of 52 and aspect of north-east. Watershed 27 has elevation from 1061 to 1454 m.a.s.l with an average slope of 55 and aspect of north-north-east. It was partially defoliated by fall crankerworm infestation from 1975 to 1979.

### 2.2. Process model

We used a parsimonious daily lumped rainfall-runoff model with quick and slow flow components "GR4J" (Modele du Genie Rural a 4 parametres Journalier) (Perrin et al., 2003), but allowed for errors at this process level. The GR4J is a modified version of the GR3J model originally proposed by Edijatno and Michel (1989) and then successively by Nascimento (1995) and Edijatno et al. (1999). We modified this model by assigning soil moisture withdrawal by evapotranspiration and percolation to 0 as soil moisture approaches the wilting point and less. We chose a lumped model instead of a spatially-explicitly distributed model because: (1) spatial variability is relatively low due to the small size of the two study watersheds; (2) subsurface processes are not well-understood, especially at the catchment scale (Perrin et al., 2003); (3) a lumped hydrological model with quick flow and slow flow components can simulate daily streamflow reasonably well (Jakeman and Hornberger, 1993); and (4) distributed models would be extremely slow within an MCMC algorithm.

The GR4J has four parameters: the maximum capacity of soil moisture storage, similar to field capacity of soil, a ground water exchange coefficient, the maximum capacity of routing storage, and a time base of a unit hydrograph (i.e., time of concentration of a watershed, defined as time required for water to travel from the most hydraulically remote point in the basin to the basin outlet). We chose Thornthwaite's method (1948) for estimating potential evapotranspiration (PET). GR4J uses its two production parameters (maximum capacities of soil moisture accounting storage and routing storage) to adapt to the various PET estimates;

thus the simple approach used to estimate watershed PET, produces the similar streamflow results as PET estimates from more complex approaches, such as eddy covariance measurements (Andréassian et al., 2004). More specifically, Oudin et al. (2004) showed that perturbation errors in the PET were absorbed by the model's production (soil moisture storage) reservoir, which controlled the water losses from the model.

The model contains four sub-models (all the units are in millimeters unless indicated otherwise):

(1) A soil moisture sub-model;

If we use  $p_t$  and  $E_t$  to denote catchment precipitation and PET respectively on day  $t$ , then

$$\begin{aligned} NP_t &= p_t - E_t \text{ and } NE_t = 0 \text{ if } p_t \geq E_t \\ NP_t &= 0 \text{ and } NE_t = E_t - p_t \text{ otherwise} \end{aligned} \quad (1)$$

where  $NP_t$  denotes net precipitation on day  $t$  and  $NE_t$  denotes net evapotranspiration on day  $t$ .

If  $NP_t$  is not zero, a part  $F_t$  of  $NP_t$  fills in the soil moisture storage:

$$F_t = \frac{k_1 \left(1 - \left(\frac{s_{t-1}}{k_1}\right)^2\right) \tanh\left(\frac{NP_t}{k_1}\right)}{1 + \frac{s_{t-1}}{k_1} \tanh\left(\frac{NP_t}{k_1}\right)} \quad (2)$$

where  $s_{t-1}$  denotes soil moisture storage level on day  $t-1$ , a parameter  $k_1$  denotes the maximum capacity of soil moisture storage.

The water that is evaporated from soil moisture storage on day  $t$  ( $SE_t$ ) is calculated as:

$$SE_t = \frac{s_{t-1} \left(2 - \frac{s_{t-1}}{k_1}\right) \tanh\left(\frac{NE_t}{k_1}\right)}{1 + \left(1 - \frac{s_{t-1}}{k_1}\right) \tanh\left(\frac{NE_t}{k_1}\right)} \quad (3)$$

Then the soil moisture level on day  $t$  ( $s_t$ ) can be updated as:

$$s_t = s_{t-1} + F_t - SE_t \quad (4)$$

Eqs. (2) and (3) result from the integration over the time step of the differential equations that have a parabolic form with terms in  $\left(\frac{s_{t-1}}{k_1}\right)^2$  (Edijatno and Michel, 1989; Perrin et al., 2003).

(2) An "effective precipitation" sub-model which uses soil moisture as input to calculate percolation and then effective precipitation (i.e., the proportion of precipitation that could contribute to streamflow);

A percolation leakage on day  $t$  ( $Perc_t$ ) from the soil moisture storage is calculated as a power function of the soil moisture content on day  $t$  (Eq. (5)):

$$Perc_t = s_t \left\{ 1 - \left[ 1 + \left( \frac{4}{9} \frac{s_t}{k_1} \right)^4 \right]^{-1/4} \right\} \quad (5)$$

Then the soil moisture content on day  $t$  becomes:

$$s_t = s_t - Perc_t \quad (6)$$

The effective rainfall on day  $t$  ( $Pr_t$ ) that reaches the routing process is given by

$$Pr_t = Perc_t + (NP_t - F_t) \quad (7)$$

(3) A sub-model that calculates slow streamflow from a non-linear routing process; and (4) a sub-model that calculates quick streamflow from non-routing process:

$Pr_t$  is divided into two flow components according to a fixed split, 90% is routed by a unit hydrograph UH1 and then a non-linear

routing storage, and the remaining 10% is routed by a single unit hydrograph UH2. With the ordinates of UH1 and UH2, we can spread effective rainfall over  $k_4$  days for non-linear routing and  $2k_4$  days for direct or quick flow, where the parameter  $k_4$  represents time base of unit hydrography UH1 (unit: days) (Perrin et al., 2003).

A groundwater exchange term  $G_t$  interacts with both non-linear routing and quick streamflow and is calculated as:

$$G_t = k_2 \left( \frac{R_{t-1}}{k_3} \right)^{7/2} \quad (8)$$

where a parameter  $k_2$  denotes exchange coefficient (unitless), a parameter  $k_3$  denotes the maximum capacity of routing storage, and  $R_{t-1}$  denotes the water level in the routing storage on day  $t-1$ .

Let  $q_{1t}$  denote the output from UH1 on day  $t$ , we update  $R_t$  as (Eq. (9)):

$$R_t = \max(0; R_{t-1} + q_{1t} + G_t) \quad (9)$$

The output of the routing reservoir on day  $t$  ( $Q_{rt}$ ) is then calculated as (Eq. (10)):

$$Q_{rt} = R_t \left\{ 1 - \left[ 1 + \left( \frac{R_t}{k_3} \right)^4 \right]^{-1/4} \right\} \quad (10)$$

Let  $q_{2t}$  denotes the output from UH2 on day  $t$ , then the direct (quick) flow on day  $t$  ( $Q_{dt}$ ) is calculated as (Eq. (11)):

$$Q_{dt} = \max(0; q_{2t} + G_t) \quad (11)$$

Additional details on the model (i.e., determining the ordinates of the unit hydrographs) are contained in Perrin et al. (2003). The model has been applied to more than 2000 catchments with different sizes in different climate regions of the world (personal communication with Andréassian Vazken, one of the model developers for GR4J), so there is prior information available for the four parameters ( $k_1$ – $k_4$ ) that require estimation.

### 2.3. Hierarchical Bayesian model

Hierarchical Bayesian models accommodate decomposing high-dimensional problems into stages within a consistent framework (Clark, 2005) including data (Eq. (12a)); process (Eq. (12b)); and parameter (Eq. (12c)).

$$\begin{aligned} p(\text{parameters, process} | \text{data, priors}) \\ \propto p(\text{data} | \text{process, data parameters}) \quad (\text{a}) \\ \times p(\text{process} | \text{process parameters}) \quad (\text{b}) \\ \times p(\text{all parameters} | \text{priors}) \quad (\text{c}) \end{aligned} \quad (12)$$

Our hierarchical model structure was designed to estimate the components of streamflow generation (Fig. 2), including the parameters, latent states of soil moisture and streamflow, and uncertainties. We assumed the major uncertainties of the model include change in soil moisture and streamflow (termed "model misspecification" or "process error"). Thus, the sub-models for soil moisture (Eqs. (1)–(4), referred as  $f_2$ ), slowflow, and quickflow (Eqs. (8)–(11), referred as  $f_1$ ) were stochastic, while the sub-model of effective precipitation (Eqs. (5)–(7)) was treated deterministically (Fig. 2A). A state-space model, which accounted for temporal dependence, was implemented for soil moisture (Fig. 2B).

Let  $q_t$  represent log streamflow at time  $t$  ( $\log(Q_{rt} + Q_{dt})$ ), which was influenced by soil moisture at time  $t$ , the routing process (Eq. (10)), non-routing processes (Eq. (11)) in the GR4J model, and lognormal error  $\sigma_1^2$ ,

$$q_t \sim N(f_1(s_t, k_2, k_3, k_4), \sigma_1^2) \quad (13)$$

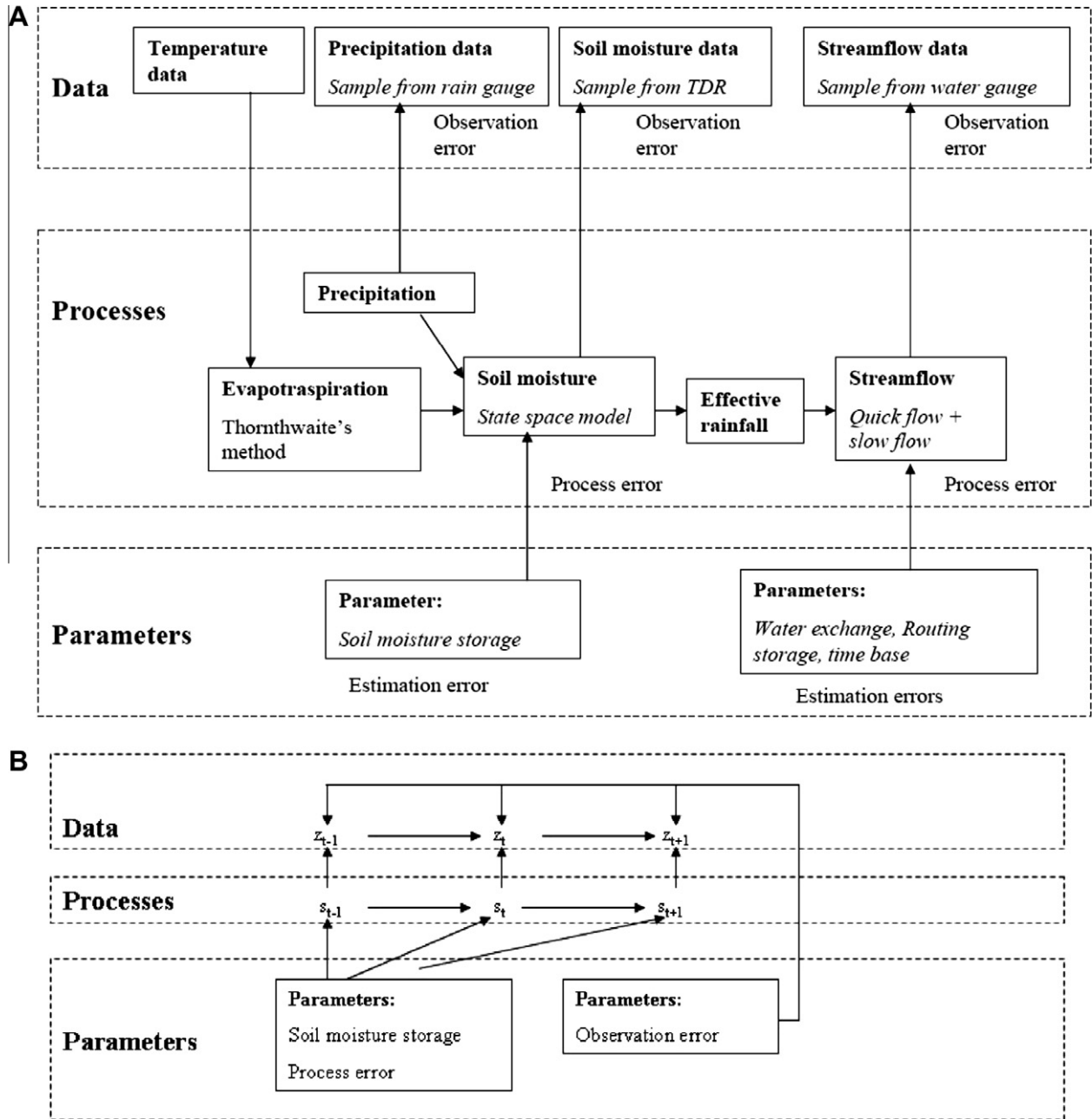


**Fig. 2.** Model structure for the hierarchical Bayes analysis based on Eq. (12) (A: boxes contain model elements. Sources of stochasticity are italics.) with the state space portion for soil moisture sub-model (B: the upper data level consists of observations  $z$ , the middle process level include the unobserved latent process  $s$ , and the parameter level contains maximum capacity of soil moisture accounting storage, and the variances for the process error and observation error. The lower two levels are not observed and must be estimated).

where “ $\sim$ ” represents “is distributed as”,  $N$  is a normal distribution, and  $k_2$ – $k_4$  are the parameters of the process model GR4J.

Soil moisture changed from time  $t-1$  to time  $t$  due to addition by precipitation  $p_t$ , losses through evapotranspiration determined by temperature  $t_t$ , and normal error  $\sigma_2^2$ ,

$$s_t \sim N(f_2(s_{t-1}, p_t, t_t, k_1), \sigma_2^2) \tag{14}$$

We considered the effects of sampling, or observation errors, for the measurements of streamflow and soil moisture. Let  $y_t$  represent the observations of log streamflow at time  $t$ ,  $z_t$  represent the observations of soil moisture at time  $t$ . The lognormal observation error model for streamflow and normal observation error model for soil moisture were:

$$y_t \sim N(q_t, \tau_1^2) \tag{15}$$

$$z_t \sim N(s_t, \tau_2^2) \tag{16}$$

For Gibbs sampling, the conditional density for streamflow at time  $t$  was:

$$p(q_t | s_t, y_t, k_2, k_3, k_4, \sigma_1^2, \tau_1^2) \propto N(q_t | f_1(s_t, k_2, k_3, k_4), \sigma_1^2) \times N(y_t | q_t, \tau_1^2) \tag{17}$$

The conditional density for soil moisture at time  $t$  (Clark and Bjørnstad, 2004) included the observation at time  $t$ ,  $z_t$ , and the state of the process immediately before and after  $t$  (i.e.,  $s_{t-1}$ , and  $s_{t+1}$ ),

$$p(s_t, |s_{t-1}, s_{t+1}, z_t, p_t, p_{t+1}, t, t_{t+1}^o, k_1, \sigma_2^2, \tau_2^2) \propto N(s_t | f_2(s_{t-1}, p_t, t, k_1), \sigma_2^2) \times N(s_{t+1} | f_2(s_t, p_{t+1}, t_{t+1}, k_1), \sigma_2^2) \times N(z_t | s_t, \tau_2^2) \tag{18}$$

The three densities on the right hand side of (18) represented the arrow pointing from  $s_{t-1}$  to  $s_t$ , the arrow pointing from  $s_t$  to  $s_{t+1}$ , and the arrow pointing from  $s_t$  to  $z_t$  in Fig. 2B.

We also assimilated the log measurement error described by variance  $\tau_p^2$  in observed precipitation  $p_t^o$ ,

$$\log(p_t^o) \sim N(\log(p_t), \tau_p^2) \tag{19}$$

We did not include measurement errors for temperature because they were small.

To complete the Bayesian model, we require prior distributions for unknown parameters. For convenience we used priors that were conjugate with the likelihood (Calder et al., 2003), such that prior and posterior distributions had the same form. The variance parameters  $\sigma_1^2, \sigma_2^2, \tau_1^2, \tau_2^2, \tau_p^2$  had inverse gamma (IG) priors, conjugate for the normal likelihood. We used “noninformative” priors, meaning that prior distributions were rather flat and only weakly influenced parameter estimates since we knew little about the model and observation errors (Hartigan, 1998; Clark and Bjørnstad, 2004). A noninformative inverse gamma density prior had parameter values that were small. Based on the previous studies, the conjugate priors for the parameters of  $k_1, k_2, k_3, k_4$  followed a multivariate log-normal distribution without covariance between parameters (20):

$$\log(k_1, k_2, k_3, k_4) \sim N(\log(B), \text{diagonal}(V_B)) \tag{20}$$

where  $B = (350, 0.0001, 90, 1.7)$ ,  $\text{diagonal}(V_B) = (0.4, 2.0, 0.1, 0.2)$  (Note: The values of  $B$  were from Perrin et al. (2003), while  $V_B$  was weakly informative)

Combining the data, process, and parameter models, we had the joint posterior

$$p(k_1, k_2, k_3, k_4, s, q, \sigma_1^2, \sigma_2^2, \tau_1^2, \tau_2^2, \tau_p^2 | p^o, t, y, z, \text{priors}) \tag{21}$$

$$\propto \prod_{t=1}^T N(y_t | q_t, \tau_1^2) \prod_{t=1}^T N(z_t | s_t, \tau_2^2) \prod_{t=1}^T N(q_t | f_1(s_t, k_2, k_3, k_4), \sigma_1^2) \prod_{t=2}^T N((s_t | f_2(s_{t-1}, p_t, t, k_1), \sigma_2^2) \prod_{t=1}^T N(\log(p_t^o) | \log(p_t), \tau_p^2) N(\log(k_1, k_2, k_3, k_4) | \log(B), \text{diagonal}(V_B)) IG(\sigma_1^2 | \alpha_{\sigma_1}, \beta_{\sigma_1}) IG(\sigma_2^2 | \alpha_{\sigma_2}, \beta_{\sigma_2}) IG(\tau_1^2 | \alpha_{\tau_1}, \beta_{\tau_1}) IG(\tau_2^2 | \alpha_{\tau_2}, \beta_{\tau_2}) IG(\tau_p^2 | \alpha_{\tau_p}, \beta_{\tau_p})$$

In order to estimate the importance of assimilating soil moisture data, we also developed a hierarchical model without assimilating soil moisture data and then we compared the predictions of streamflow from both models.

2.4. Model implementation

The initial values for the water levels of the two storage components (soil moisture storage and routing storage) were estimated based on the initial values of  $k_1, k_3$  (Edijatno et al., 1999). TDR soil moisture data were expressed as a percentage of volume whereas

**Table 1** Summary of posterior distributions of the four process parameters for Watershed 18 (the column of “SM” represents the results from the Bayesian model assimilating soil moisture data, and the column of “NO SM” represents those from the model not assimilating soil moisture data).

Parameters	Mean		Median		Lower 2.5% quantile		Upper 2.5% quantile	
	SM	NO SM	SM	NO SM	SM	NO SM	SM	NO SM
$k_1$ (mm)	280	825	280	819	277	730	283	935
$k_2$ (unitless)	0.0017	0.00034	0.00088	0.00012	0.000078	0.000015	0.0083	0.0019
$k_3$ (mm)	738	378	737	382	672	294	810	466
$k_4$ (day)	0.82	0.64	0.82	0.63	0.75	0.51	0.90	0.82

**Table 2** Summary of posterior distributions of the four process parameters for Watershed 27 (the column of “SM” represents the results from the Bayesian model assimilating soil moisture data, and the column of “NO SM” represents those from the model not assimilating soil moisture data).

Parameters	Mean		Median		Lower 2.5% quantile		Upper 2.5% quantile	
	SM	NO SM	SM	NO SM	SM	NO SM	SM	NO SM
$k_1$ (mm)	194	550	194	548	190	482	197	627
$k_2$ (unitless)	0.0020	0.0015	0.00010	0.00083	0.000072	0.000083	0.0095	0.0078
$k_3$ (mm)	266	145	266	144	236	123	300	170
$k_4$ (day)	0.82	0.85	0.82	0.85	0.73	0.67	0.93	0.99

**Table 3** Summary of posterior distributions of the four process parameters for Watershed 18 (WS18) and 27 (WS27) when soil moisture data were assimilated but the observation errors of precipitation were not accounted for.

Parameters	Mean		Median		Lower 2.5% quantile		Upper 2.5% quantile	
	WS18	WS27	WS18	WS27	WS18	WS27	WS18	WS27
$k_1$ (mm)	282	194	282	196	274	190	289	201
$k_2$ (unitless)	0.0026	0.0016	0.00083	0.0016	0.00014	0.00422	0.0064	0.00527
$k_3$ (mm)	677	266	675	262	600	229	762	303
$k_4$ (day)	0.82	0.82	0.82	0.82	0.69	0.70	0.94	0.96

most hydrological models use the unit of mm or cm. Hence, we converted TDR based percentage measurements to soil water con-

tent in mm (i.e., percentage  $\times$  soil depth) in the upper 60 cm soil layer.

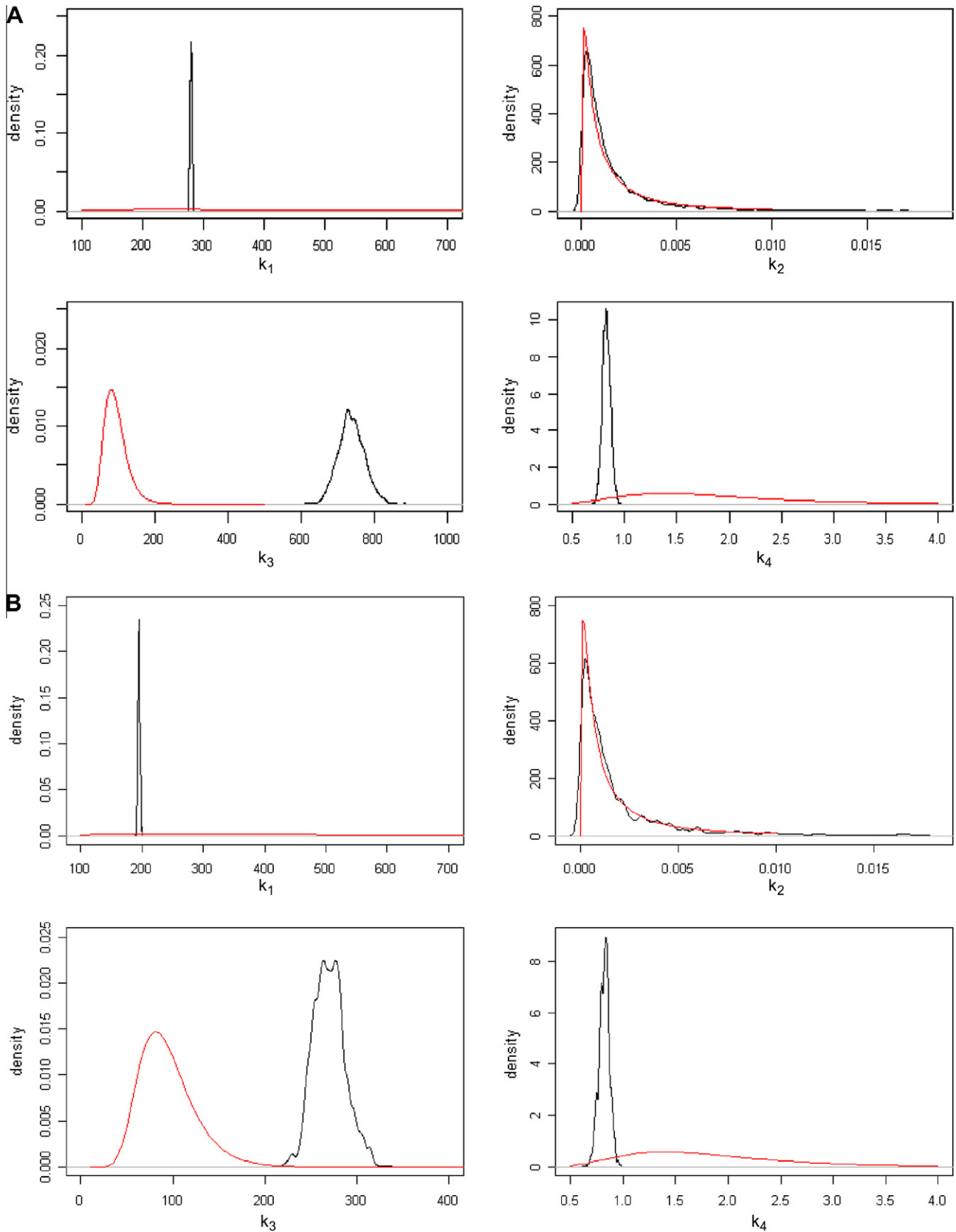


**Fig. 3.** Prior (red) and posterior (black) density probability distributions of the four parameters at Watershed 18 (the upper four, A) and 27 (the lower four, B). (Units:  $k_1$ , mm;  $k_2$ , unitless;  $k_3$ , mm;  $k_4$ , days.)

We implemented MCMC in R (R development core team, 2008) for observations from 1999 to 2002. The algorithm included Gibbs sampling and adaptive Metropolis–Hastings steps (Haario et al., 2001; Marshall et al., 2004) to draw samples alternatively from the conditional posteriors for each of the unknowns, including the latent variables and parameters (Clark and Bjørnstad, 2004). The adaptive algorithm is characterized by a proposal distribution based on the estimated posterior covariance matrix of the parameters, which is updated automatically. The posterior covariance matrix is calculated based on past iterations.

### 2.5. Model diagnosis

We evaluated convergence by simulating Markov chains from different starting values and multiple chains. Convergence required 1000–5000 iterations. These pre-convergence “burn-in”

iterations were discarded and an additional 10,000 iterations were saved for the analysis.

## 3. Results and discussion

### 3.1. Posteriors from the Bayesian models

The posteriors of the exchange coefficient ( $k_2$ ) for both watersheds were close to 0, consistent with the previous knowledge of impervious bottom of the soil layer, preventing water from exchanging between the vadose zone and ground water (Tables 1 and 2). The posteriors for the maximum capacity of accounting storage ( $k_1$ ) and routing storage ( $k_3$ ) at the low elevation Watershed 18 were larger than those at the high elevation Watershed 27. This is consistent with a decrease in soil depth with elevations (Swank and Crossley Jr., 1988). The posteriors of the time base of

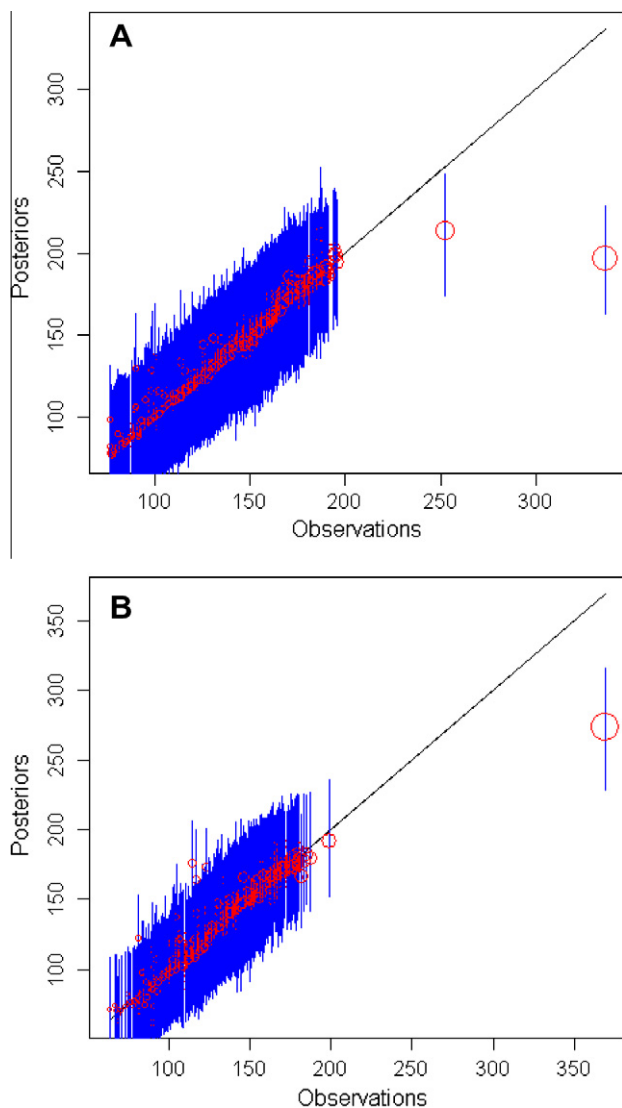


**Fig. 4.** Comparison between measured and posterior medians of the soil moisture levels (mm) at the upper 60 cm soil during the calibration period (2000–2002) at Watershed 18 (A) and at Watershed 27 (B). The centers of the red circles correspond to posterior medians at Y-axis and measurements at X-axis. The sizes of the red circles are proportional to the measurements. Blue bars represent 95% credible intervals (lower 2.5% quantiles–upper 2.5% quantiles) of the posteriors. The black line represents 1:1 line. The closer the red circles and blue bars to the 1:1 line, the better the model simulations are. (For interpretation of the references to colour in this figure legend, the reader is referred to the web version of this article.)

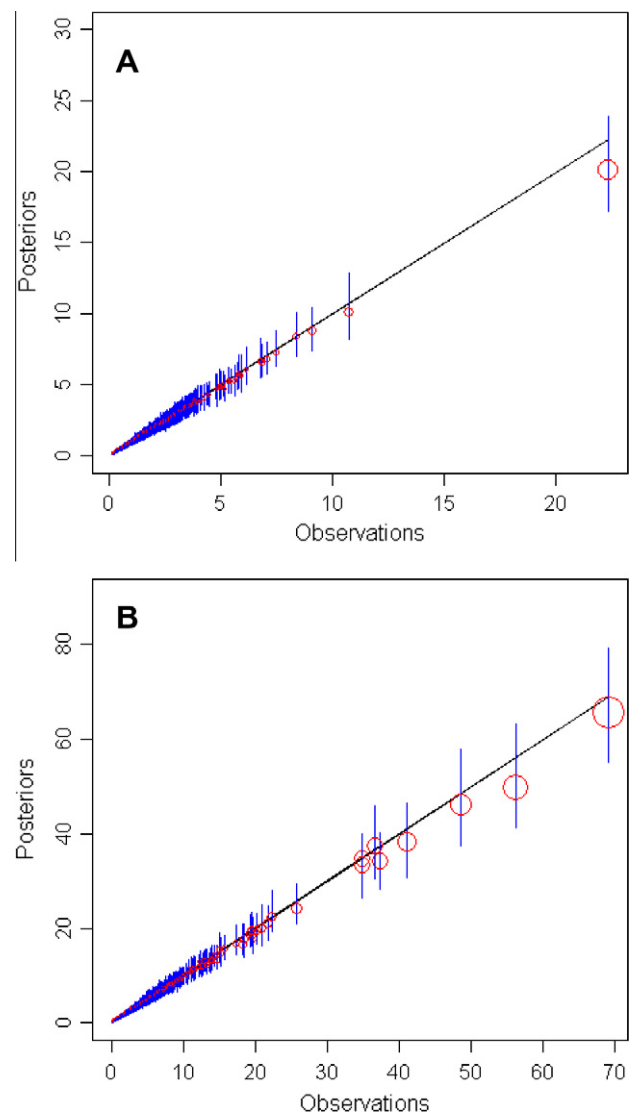


**Fig. 5.** Comparison between measured and posterior medians of streamflow (mm) during the calibration period (2000–2002) at Watershed 18 (A) and 27 (B). The centers of the red circles correspond to posterior medians at Y-axis and measurements at X-axis. The sizes of the red circles are proportional to the measurements. Blue bars represent 95% credible intervals (lower 2.5% quantiles–upper 2.5% quantiles) of the posteriors. The black line represents 1:1 line. The closer the red circles and blue bars to the 1:1 line, the better the model simulations are. (For interpretation of the references to colour in this figure legend, the reader is referred to the web version of this article.)

the unit hydrograph ( $k_4$ ) for both watersheds were less than 1 day, most likely due to the small size of the watersheds (Tables 1 and 2). The upper 2.5% quantile of the posteriors of  $k_4$  from the model assimilating soil moisture data was larger at Watershed 27 than at Watershed 18. The same applied to the median, mean, lower and upper 2.5% quantiles of the posteriors of  $k_4$  from the model

not assimilating soil moisture data, likely due to that Watershed 27 is three times as large as Watershed 18.

Assimilation of soil moisture data increased precision of estimates of the maximum capacity of soil moisture storage  $k_1$  (277–283 mm at Watershed 18 and 190–197 mm at Watershed 27 by assimilating soil moisture data, 730–935 mm at Watershed 18

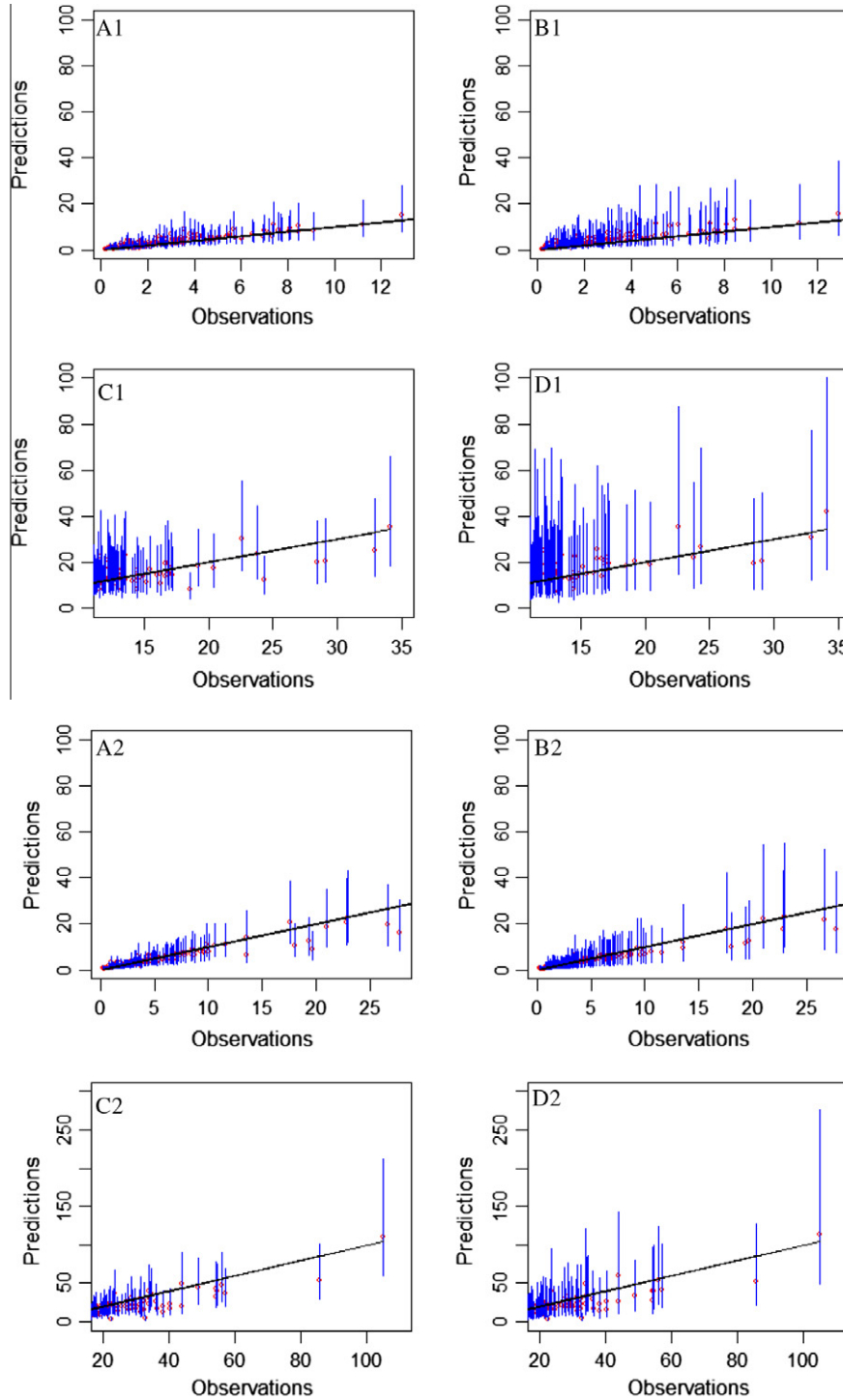


**Fig. 6.** Streamflow (mm) predictions by assimilating soil moisture data (A and C) and not assimilating soil moisture data (B and D) at Watershed 18 between 1986 and 1999 (1) and at Watershed 27 between 1994 and 1999 (2). We did not include the predictions of the first years for both watersheds to avoid the effect of initial values for the water levels of soil moisture and routing storage. The centers of the red circles correspond to medians at Y-axis and measurements at X-axis. Blue bars represent 95% credible intervals (lower 2.5% quantiles–upper 2.5% quantiles) of the predictions. The black line represents 1:1 line. The closer the red circles and blue bars to the 1:1 line, the better the model simulations are. Since the time step in the predictions is daily, we plotted the predictions every 30 days (A1 and B1) for Watershed 18 and every 15 days for Watershed 27 (A2 and B2). The larger streamflow predictions which were missing from A and B were represented in C and D. (For interpretation of the references to colour in this figure legend, the reader is referred to the web version of this article.)

and 482–627 mm at Watershed 27 when not assimilating them). There were two other differences if the soil moisture data were

not assimilated compared to the model with soil moisture data: (1) the estimated maximum capacity of the soil moisture storage

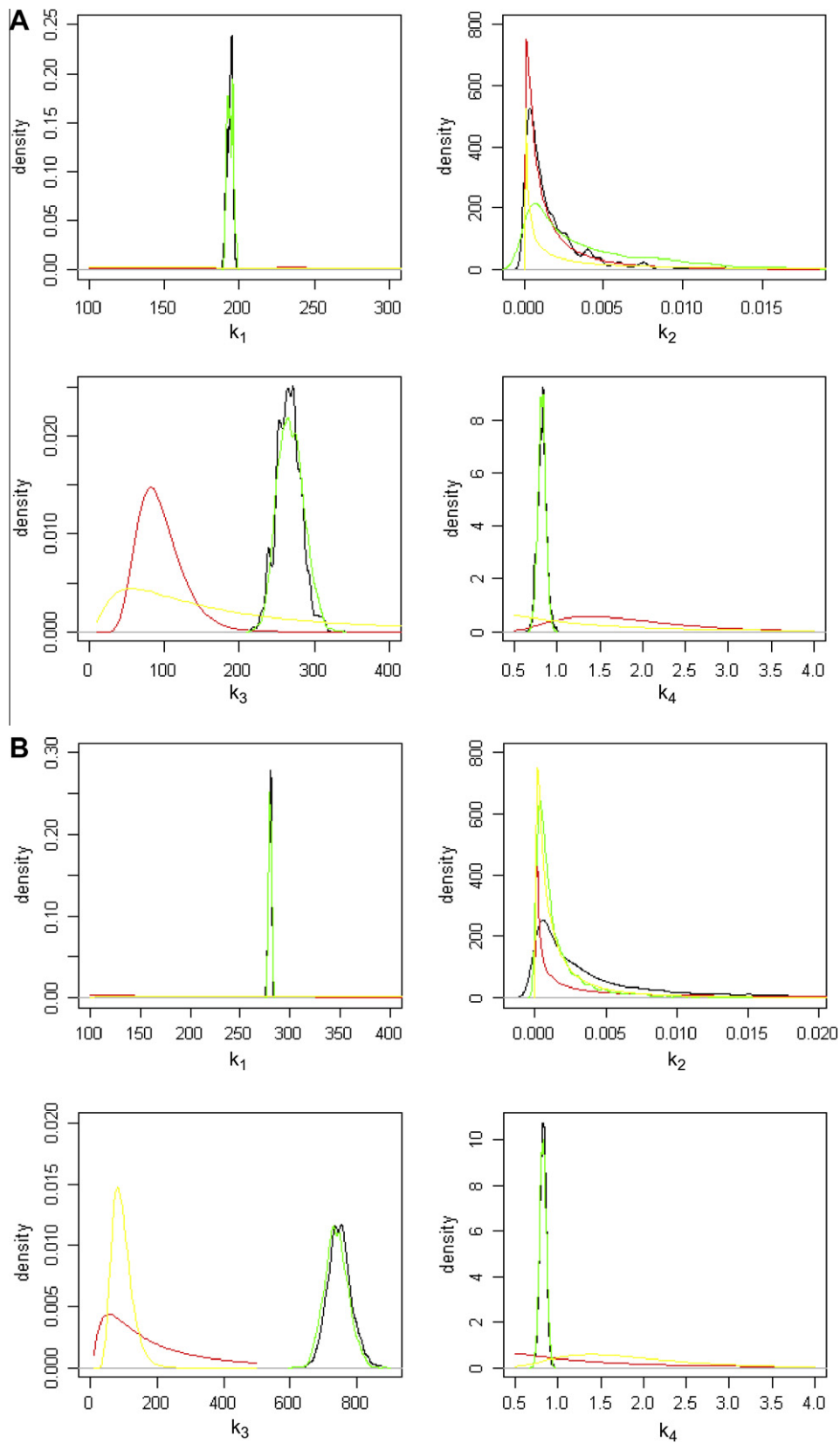


Fig. 7. The sensitivity of the posterior distribution to the prior distribution for the four parameters (prior1: red; posteriors using prior1: black; prior2: yellow; posteriors using prior2: green) at Watershed 18 (the upper four, A) and 27 (the lower four, B). (Units:  $k_1$ , mm;  $k_2$ , unitless;  $k_3$ , mm;  $k_4$ , days.)

was larger, and (2) the estimated maximum capacity of routing storage was smaller (Tables 1 and 2). The estimated maximum capacity of soil moisture storage from the model that included soil moisture data was for the upper 60 cm. If the soil moisture measurements were not included, the estimated maximum capacity of soil moisture storage applied to the entire soil depth, and thus was larger and had greater variance. In addition the maximum capacity of soil moisture storage and maximum capacity of routing storage had compensating effects.

The difference of the parameter estimates between the simulations accounting for and not accounting for observation errors of precipitation were small except for  $k_3$  at Watershed 18 (Table 3). With the exception of  $k_2$ , credible intervals were larger when observation errors were ignored. We expect that the benefit of assimilating observation errors will increase for larger watersheds with higher spatial variability (Kavetski et al., 2006a,b).

With the exception for the exchange coefficient ( $k_2$ ), the prior and posterior distributions differed substantially for the process parameters. Posterior modes for  $k_1$ ,  $k_3$ , and  $k_4$  had low prior probabilities, indicating they were mainly determined by data at both watersheds (Fig. 3). The prior and posterior distributions of  $k_2$  were close, implying that the prior played a significant role in determining posterior. The sensitivity of posteriors to priors was discussed later in the paper.

The posterior medians of the soil moisture levels from the state-space model were close to the measured data for observed values <250 mm for both watersheds (Fig. 4). The model underestimated soil moisture level at higher levels. The extremely large values of the soil moisture measurements could be due to measurement errors as the observations did not fall within the credible intervals of the posteriors.

Generally, the posterior medians of streamflow from the model for both watersheds followed the measured streamflow, and the streamflow observations fell within the credible interval of the streamflow posteriors (Fig. 5). The model tended to under-estimate streamflow when the measured daily streamflow was >40 mm/day.

### 3.2. Streamflow predictions

Bayesian posteriors can be used for prediction. The posteriors are probability-based, as are predictions. We applied the model and the posteriors of the parameters and variances for different times (1985–1999 for Watershed 18 and 1993–1999 for Watershed 27) from that used to generate the posteriors, and estimated the predictive intervals for streamflow to assess the predictability of the GR4J model. We compared the predictions from the model assimilating soil moisture data with those from the one that did not (Fig. 6). The predicted medians of streamflow at both watersheds followed the measurements closely, with under-estimates when it was >25 mm at Watershed 27, and overestimates when it was <10 mm at Watershed 18 (Fig. 6). The streamflow measurements all fell within the predictive intervals. The over- and under-estimations were due to the uncertainties involved in model parameters, model, and observations.

Soil moisture integrates many of the biological and physical processes that regulate streamflow, including precipitation, water uptake, soil texture, and other soil physical attributes, so streamflow can be predicted with higher precision if soil moisture data is assimilated, especially during storm events (e.g. streamflow observations > 5 mm/day). Although our model still tended to over- or under-estimate streamflow for certain days when the soil moisture observations were assimilated, the extent of over- and under-estimations were not as large (Fig. 6) compared to the model without soil moisture data. This finding is further evidence that assimilation of soil moisture is particularly effective during storm

events, as suggested from previous Kalman filter results (Aubert et al., 2003).

### 3.3. Sensitivity of posteriors to priors

All inference is subjective. Bayesians make the subjectivity explicit, through tractable prior parameter values. In a classical setting, many aspects of data modeling that need careful thought are not apparent, fostering the “illusion of objectivity” (Berger and Berry, 1988; Clark, 2007). A posterior may be robust to different priors. The sensitivity of the posteriors to the prior assumptions can be explored by changing the priors (Clark, 2007).

We explored two sets of priors for the four process parameters, both were multivariate log-normal distributions but differed in their mean values. One set, based on Perrin et al. (2003), was used for our simulations in Section 3.1 (prior 1), the other set was derived from watershed size and long term annual temperature according to Kuczera and Parent (1998) (prior 2). From the sensitivity analysis at both watersheds, the posterior distributions of  $k_1$ ,  $k_3$  and  $k_4$  were not sensitive to priors, and mainly determined by data (Fig. 7). The posterior for  $k_2$  was sensitive to the prior specification. From previous studies of the GR4J model and our knowledge of Coweeta Basin, a prior mean value for  $k_2$  close to 0 was consistent with posterior inference. The prior and posteriors of  $k_1$ ,  $k_3$  and  $k_4$  were well displaced from one another, which may be due to the fact that the hydrological conditions at Coweeta Basin differ from those where the model was applied before.

## 4. Conclusion

By applying Bayesian inference, we were able to assimilate uncertainties associated with parameters, observations and model structures, and to determine the value of soil moisture data for streamflow prediction. The parsimonious model GR4J can be used for meaningful prediction. By assimilating both soil moisture and streamflow measurements, we achieved a more precise prediction for streamflow, especially during storm events.

The coherent assimilation of uncertainties in hydrological models using hierarchical Bayesian models not only provides better scientific understanding on hydrological cycles and admits the field data needed to reduce the prediction errors (e.g. soil moisture data), but also presents more useful information than point estimates to facilitate water resource planning and management by acknowledging stochasticity.

## Acknowledgements

This research was made possible by grants from the National Science Foundation (NSF) through Coweeta Long Term Ecological Research (LTER). We thank USDA-Forest Service Coweeta Hydrologic Laboratory for the support of the data. We thank Drs. Chelcy Ford and Katherine Elliott at Coweeta Hydrological Laboratory for the insightful discussion on hydrological cycles at Coweeta Basin. We especially thank Dr. Jerry Mead at the Academy of Natural Sciences for critical review. We are also very grateful for two anonymous reviewers and the editor for their constructive comments and suggestions to help improve the manuscript.

## References

- Andréassian, V., Perrin, C., Michel, C., 2004. Impact of imperfect potential evapotranspiration knowledge on the efficiency and parameters of watershed models. *Journal of Hydrology* 286, 19–35.
- Aubert, D., Loumagne, C., Oudin, L., 2003. Sequential assimilation of soil moisture and streamflow data in a conceptual rainfall-runoff model. *Journal of Hydrology* 280, 145–161.

- Bates, B.C., Campbell, E.P., 2001. A Markov chain Monte Carlo scheme for parameter estimation and inference in conceptual rainfall-runoff modeling. *Water Resources Research* 37 (4), 937–947.
- Berger, J., Berry, D., 1988. Statistical analysis and the illusion of objectivity. *American Scientist* 76, 159–165.
- Blume, T., Zehe, E., Bronstert, A., 2007. Use of soil moisture dynamics and patterns for the investigation of runoff generation processes with emphasis on preferential flow. *Hydrology and Earth System Sciences and Discussions* 4, 2587–2624.
- Calder, K., Lavine, M., Mueller, P., Clark, J.S., 2003. Incorporating multiple sources of stochasticity in population dynamic models. *Ecology* 84, 1395–1402.
- Campbell, E.P., Fox, D.R., Bates, B.C., 1999. A Bayesian approach to parameter estimation and pooling in nonlinear flood event models. *Water Resources Research* 35 (1), 211–220.
- Clark, J.S., 2005. Why environmental scientists are becoming Bayesians. *Ecology Letters* 8, 2–14. doi:10.1111/j.1461-0248.2004.00702.x.
- Clark, J., 2007. *Models for Ecological Data*. Princeton University Press, 617p.
- Clark, J.S., Bjørnstad, O.N., 2004. Population time series: process variability, observation errors, missing values, lags, and hidden states. *Ecology* 85 (11), 3140–3150.
- Clark, J.S., Carpenter, S.R., Barbar, M., Collins, S., Dobson, A., Foley, J.A., Lodge, D.M., Pascual, M., Pielke Jr., R., Pizer, W., Pringle, C., Reid, W.V., Rose, K.A., Sala, O., Schlesinger, W.H., Wall, D.H., Wear, D., 2001. Ecological forecasts: an emerging imperative. *Science* 293, 657–660.
- Edijatno, Michel, C., 1989. Un modèle pluie-débit journalier à trois paramètres. *La Houille Blanche* 2, 113–121.
- Edijatno, Nascimento, N.O., Yang, X., Makhlof, Z., Michel, C., 1999. GR3J: a daily watershed model with three free parameters. *Hydrological Sciences Journal* 44 (2), 263–277.
- Haario, H., Saksman, E., Tamminem, J., 2001. An adaptive Metropolis algorithm. *Bernoulli* 7 (2), 223–242.
- Hartigan, J.A., 1998. The maximum likelihood prior. *Annals of Statistics* 26, 2083–2103.
- Hatcher Jr., R.D., 1979. The Coweeta Group and Coweeta syncline: major features of the North Carolina – Georgia Blue Ridge. *Southeastern Geology* 21 (1), 17–29.
- Hatcher Jr., R.D., 1988. Bedrock geology and regional geologic setting of Coweeta Hydrologic Laboratory in the eastern Blue Ridge. In: Swank, W.T., Crossley, D.A., Jr. (Eds.), *Forest Hydrology and Ecology at Coweeta*. Ecological Studies. Springer-Verlag, New York, pp. 81–92.
- Jakeman, A., Hornberger, G., 1993. How much complexity is warranted in a rainfall-runoff model? *Water Resources Research* 29 (8), 2637–2649.
- Kavetski, D., Kuczera, G., Franks, S.W., 2006a. Bayesian analysis of input uncertainty in hydrological modeling: 1. Theory. *Water Resource Research* 42, W03407. doi:10.1029/2005WR004368.
- Kavetski, D., Kuczera, G., Franks, S.W., 2006b. Bayesian analysis of input uncertainty in hydrological modeling: 2. Application. *Water Resource Research* 42, W03408. doi:10.1029/2005WR004376.
- Kienzler, P.M., Naef, F., 2007. Temporal variability of subsurface stormflow formation. *Hydrology and Earth System Sciences and Discussions* 4, 2143–2167.
- Kuczera, G., Mroczkowski, M., 1998. Assessment of hydrologic parameter uncertainty and the worth of multiresponse data. *Water Resources Research* 34 (6), 1481–1489.
- Kuczera, G., Parent, E., 1998. Monte Carlo assessment of parameter uncertainty in conceptual catchment models: the metropolis algorithm. *Journal of Hydrology* 211, 69–85.
- Mantovan, P., Todini, E., 2006. Hydrological forecasting uncertainty assessment: incoherence of the GLUE methodology. *Journal of Hydrology* 330, 368–381.
- Marshall, L., Nott, D., Sharma, A., 2004. A comparative study of Markov chain Monte Carlo methods for conceptual rainfall-runoff modeling. *Water Resources Research* 40. doi:10.1029/2003WR002378.
- Nascimento, N.O., 1995. *Appréciation à l'aide d'un modèle empirique des effets d'action anthropiques sur la relation pluie-débit à l'échelle du bassin versant*. Ph.D. Thesis, CERGRENE/ENPC, Paris, France, 550pp.
- Oudin, L., Andréassian, V., Perrin, C., 2004. Locating the sources of low-pass behavior within rainfall-runoff models. *Water Resources Research* 40, W11101. doi:10.1029/2004WR003291.
- Perrin, C., Michel, C., Andréassian, V., 2003. Improvement of a parsimonious model for streamflow simulation. *Journal of Hydrology* 279, 275–289.
- R Development Core Team, 2008. *R: A Language and Environment for Statistical Computing*. R Foundation for Statistical Computing, Vienna, Austria. ISBN 3-900051-07-0. <<http://www.R-project.org>>.
- Swank, W.T., Crossley Jr., D.A., 1988. *Forest Hydrology and Ecology at Coweeta*. Ecological Studies, vol. 66. Springer-Verlag, New York.
- Swift Jr., L.W., Cunningham, G.B., Douglass, J.E., 1988. *Climatology and hydrology*. In: Swank, W.T., Crossley, D.A., Jr. (Eds.), *Forest Hydrology and Ecology at Coweeta*. Ecological Studies, vol. 66. Springer-Verlag, New York, pp. 35–55.
- Thorntwaite, C.W., 1948. An approach toward a rational classification of climate. *Geographical Review* 38 (1), 55–94.
- Van Meerveld, I.T., McDonnell, J.J., 2005. Comment to “Spatial correlation of soil moisture in small catchments and its relationship to dominant spatial hydrological processes”. *Journal of Hydrology* 286, 113–134. *Journal of Hydrology* 303, 307–312.
- Western, A.W., Zhou, S., Grayson, R.B., McMahon, T.A., Blöschl, G., Wilson, D.J., 2004. Spatial correlation of soil moisture in small catchments and its relation to dominant spatial hydrological processes. *Journal of Hydrology* 286, 113–134.